Philosophical Magazine

ISSN: 1478-6435 (Print) 1478-6443 (Online) Journal homepage: http://www.tandfonline.com/loi/tphm20

Abrikosov-to-Josephson vortex lattice crossover in heavy fermion $CeCoIn_5$

H. A. Radovan , T. P. Murphy , E. C. Palm , S. W. Tozer , J. C. Cooley , I. Mihut & C. C. Agosta

To cite this article: H. A. Radovan , T. P. Murphy , E. C. Palm , S. W. Tozer , J. C. Cooley , I. Mihut & C. C. Agosta (2006) Abrikosov-to-Josephson vortex lattice crossover in heavy fermion $CeCoIn_5$, Philosophical Magazine, 86:23, 3569-3579, DOI: 10.1080/14786430600672703

To link to this article: https://doi.org/10.1080/14786430600672703

Published online: 21 Feb 2007.

Philosophical Magazine,
Vol. 86, No. 23, 11 August 2006, 3569–3579

Taylor & Francis
Taylor & Francis Group

Abrikosov-to-Josephson vortex lattice crossover in heavy fermion $CeCoIn_5$

H. A. RADOVAN*†, T. P. MURPHY‡, E. C. PALM‡, S. W. TOZER‡, J. C. COOLEY§, I. MIHUT¶ and C. C. AGOSTA‖

†Department of Physics, University of Puerto Rico, Mayagüez, PR 00680, USA
‡NHMFL, Florida State University, Tallahassee, FL 32310, USA
§Los Alamos National Laboratory, MST-6, Los Alamos, NM 87545, USA
¶NHMFL, Los Alamos National Laboratory, Los Alamos, NM 87545, USA
‖Department of Physics, Clark University, Worcester, MA 01610, USA

(*Received 30 November 2005; in final form 3 March 2006*)

We present torque magnetization measurements on the quasi-2D heavy fermion superconductor $CeCoIn_5$ at temperatures down to 20 mK and magnetic fields up to 18 T. At orientations with the magnetic field perpendicular to the conducting planes, a prominent vortex lattice peak effect is present at around $0.5H_{c2}$. The peak effect gradually disappears upon rotating the field into the plane parallel orientation. We interpret the absence of the peak effect for the plane parallel case as a transformation of the Abrikosov lattice into a Josephson vortex state, favored by the Pauli paramagnetic limit in $CeCoIn_5$ together with the unusually large condensation energy. Additionally, we do not observe flux avalanches as found in organic superconductors and suggest that the complete absence of vortex activity in the plane parallel field orientation is crucial for the formation of Fulde–Ferrell–Larkin–Ovchinnikov superconductivity in $CeCoIn_5$.

1. Introduction

Anisotropic superconductors in external magnetic fields are known to produce a variety of different vortex states depending largely on electronic anisotropy, temperature and applied field. Four basic energy scales govern vortex behaviour in layered type-II superconductors: (i) in-plane vortex–vortex interactions, (ii) interlayer coupling, (iii) pinning energy, and (iv) thermal fluctuations. The competition of these energy scales results in vortex lattice phases having a dimensionality ranging from 0D to 3D [1]. With increasing temperature and/or field there may exist a condition where the vortices are able to optimally adapt to the underlying pinning potential, causing the critical current and hence the magnetization to attain a local maximum. One manifestation of this competition of energy scales is the so-called peak effect (PE), sometimes referred to as fishtail effect due to the shape of the magnetic hysteresis. Although the first observation of the peak effect in niobium goes back to 1962 [2], the microscopic mechanism is still under debate [3].

*Corresponding author. Email: hradovan@uprm.edu

Philosophical Magazine
ISSN 1478–6435 print/ISSN 1478–6443 online © 2006 Taylor & Francis
http://www.tandf.co.uk/journals
DOI: 10.1080/14786430600672703

In phenomenological and simplified terms, the PE may be thought of as a transition from an ordered to a disordered vortex state. For isotropic superconductors in an increasing field, the vortex lines initially thread straight through the material. At higher fields, a disorder driven phase transition leads to plastic-like behaviour where these Abrikosov vortices bend to find an energy minimum in the surrounding potential landscape resulting in an increase of the critical current. For strongly anisotropic, layered superconductors in low fields perpendicular to the conducting planes, Abrikosov flux lines decompose into stacks of so-called pancake vortices [4]. For isotropic superconductors, Josephson interlayer coupling dominates, while for anisotropic superconductors, the much weaker interlayer coupling is predominantly electro-magnetic in origin. This electro-magnetic coupling aligns the pancakes in adjacent layers into stacks that readily decouple in increasing fields. This decoupling transition can also lead to better pinning, resulting in a peak effect for pinning sensitive measurements. Due to the weaker nature of the pancake stack coupling, one expects the peak effect to occur at lower fields. Indeed, while the PE in conventional superconductors generally occurs close to H_{c2}, in high-T_c superconductors it appears far below H_{c2}, even closer to H_{c1} in the most anisotropic systems [5, 6].

The vortex state in strongly anisotropic superconductors in fields parallel to the conducting planes is quite different in nature [7]. In plane parallel fields, the magnetic flux is concentrated in the regions between the layers forming coreless Josephson vortices, which in the most extreme decoupled situation are entirely confined in the space between two adjacent conducting layers. Vortex states at small field angles out of the planes may constitute a mixture of the Abrikosov and Josephson state, with individual pancake vortices in adjacent conducting layers building a staircase structure coupled by Josephson vortices within the less conducting layers (so-called kinked vortices). Under such anisotropic conditions in increasing applied fields at small tilt angles the flux can stay locked-in between the conducting sheets. This so-called vortex lock-in state produces an angle between internal induction and external field. Experiments on high-T_c superconductors provide evidence for all the vortex states discussed above [8].

Magnetization studies can provide a great deal of information about the anisotropy of the host crystal structure, pinning behaviour, and vortex lattice structure and dimensionality. We applied the vortex phenomenology to a study of the magnetization as a function of applied field on the heavy fermion superconductor $CeCoIn_5$ ($T_c = 2.3\,K$) [9]. The assumed proximity to an antiferromagnetic quantum critical point is held responsible for many unusual features discovered in this material, e.g. non-Fermi liquid behaviour and the possibility of a magnetically mediated pairing mechanism. The tetragonal structure is composed of two building blocks, $CeIn_3$ and $CoIn_2$, stacked sequentially along the crystallographic c-direction ($\|$ [001]); it is assumed that the $CeIn_3$ layer is responsible for superconductivity. The electronic anisotropy is largely determined by the hybridization between the Ce-4f and the Co-3d orbital. Recent band structure calculations suggest that very weak hybridization exists, which implies a rather two-dimensional structure [10]. One way to quantify the anisotropy, ε, is the out-of-plane to in-plane ratio of effective masses, $\varepsilon = (m_{c,eff}/m_{ab,eff})^{1/2} \sim \lambda_c/\lambda_{ab}$, with λ being the London penetration depth. In $CeCoIn_5$ reported values for the effective masses in different orientations range from 5 to 87 times the bare electron mass [11], yielding a rough estimate of $\varepsilon \sim 3$–4.

For comparison, $YBa_2Cu_3O_7$ (YBCO) has $\varepsilon \sim 5$, while strongly anisotropic $Bi_2Sr_2CaCu_2O_8$ and molecular superconductor systems yield $\varepsilon \sim 100$–200. Hence, at least from this viewpoint, one would expect $CeCoIn_5$ to show similar vortex properties as YBCO. However, $CeCoIn_5$ is markedly different from YBCO in the following ways. $CeCoIn_5$ is the first superconductor clearly showing Pauli paramagnetic limitation with fields parallel to the conducting planes. Typically, in superconductors in increasing magnetic fields, orbital motion of the Cooper pairs (vortices) eventually destroys the superconducting state. In the Pauli paramagnetic limit, superconductivity is destroyed when the field is strong enough to break up the pairs and align their spins, without involving Abrikosov vortices. In this limit, the upper critical field is given by the relation $H_{c2}{}^{ab}(0) = H_p(0) = \Delta_0/\sqrt{2}\mu_B$, with the Pauli limit H_p, the superconducting energy gap at zero temperature, Δ_0, and the Bohr magneton, μ_B [12]. The ratio of the parallel to the perpendicular critical field hence is given by $H_p/H_{c2}{}^c \sim \xi_{ab}/k_F^{-1}$, with ξ the coherence length and k_F the Fermi wave vector. Another difference between $CeCoIn_5$ and YBCO are the heavy electron masses in the former that counteract orbital motion and help the Pauli limit to dominate over the orbital limit. Finally, generating Abrikosov vortices with normal cores inside superconducting layers costs energy. The higher the condensation energy, the more energy is required to create the vortices. According to the BCS theory, the condensation energy at zero temperature is given by $U_s(0)$–$U_n(0) = -0.5 \cdot N(0) \cdot \Delta^2(0)$, where N is the density of states and Δ the energy gap. As the discontinuity in the zero field specific heat, $\Delta C/\gamma T_c$ (γ: Sommerfeld coefficient), is proportional to the coupling strength, which is proportional to the energy gap within the extended BCS theory, the size of $\Delta C/\gamma T_c$ is a direct measure for the condensation energy. The (weak-coupling) BCS theory derives $\Delta C/\gamma T_c = 1.43$, YBCO has $\Delta C/\gamma T_c \approx 2.5$ [13], while the molecular superconductor κ-$(BEDT\text{-}TTF)_2Cu(NCS)_2$ has $\Delta C/\gamma T_c \approx 2.8$ [14]. Heavy fermion $CeCoIn_5$, however, was found to exhibit an exceptionally large discontinuity of $\Delta C/\gamma T_c \approx 5$ [15]. This large jump in the specific heat indicates a strong decrease of the entropy at the superconducting phase transition that was interpreted as evidence for spin fluctuation-mediated superconductivity with strong fermion–boson coupling [16]. These considerations suggest that the formation of vortices in $CeCoIn_5$ requires more energy than in YBCO and, hence, should additionally hinder vortex movement across the conducting layers. Regarding these differences, particularly the Pauli limit, one might expect that the vortex state in $CeCoIn_5$ for the plane parallel field orientation should be different than found in YBCO.

2. Torque magnetization results and discussion

2.1. *Magnetization at different temperatures*

The torque cantilever setup is an established technique used to study vortex behaviour, such as hysteresis, avalanches, pinning and melting transitions, e.g. in YBCO [17] or κ-$(BEDT\text{-}TTF)_2Cu(NCS)_2$ [18]. We use a torque cantilever setup consisting of a fixed Cu reference plate and a flexible 13-μm thick Be–Cu cantilever

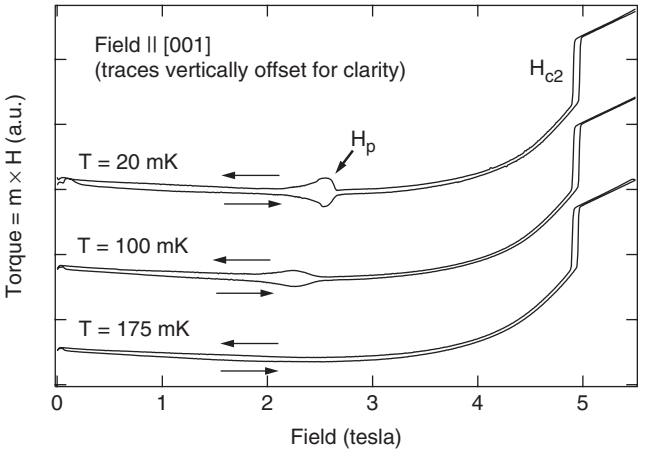

Figure 1. Torque measurements as a function of applied field perpendicular to the conducting planes of $CeCoIn_5$ at different temperatures. The arrows indicate the field sweep direction and the curves are vertically offset for clarity. The sharp transition at 5 T denotes the upper critical field, H_{c2}, while the small feature around 2.5 T, H_p, is identified as a vortex lattice peak effect.

beam with a gap of approximately 0.5 mm. We achieved similar results with a 51-μm thick Ph–Bronze cantilever and can therefore exclude material artifacts in the present data. Any magnetic moment, **m**, within a sample attached to the cantilever beam in a non-parallel magnetic field, **H**, exerts a torque on the cantilever, $\tau = \mathbf{m} \times \mathbf{H}$. The torque changes the distance of the two capacitor plates and, hence, the capacitance. The recorded signal is, therefore, proportional to the magnetization in the sample. The present torque measurements were performed at temperatures in the range 20–200 mK and fields up to 18 T (tesla) in a toploading dilution refrigerator at the NHMFL in Tallahassee, Florida. The single crystal $CeCoIn_5$ sample with lateral dimensions of $2.0 \times 1.0\,mm^2$ and 140 μm thickness was attached with GE varnish coplanar onto the cantilever beam. To exclude artifacts resulting from the specific sample geometry, we also mounted the sample on edge and obtained similar data. Since the sample had been grown from an In flux, we etched it prior to mounting in an $HCl/HNO_3/H_2O$ (3:1:10, v/v) solution for about 10 min to remove excess indium.

Figure 1 presents torque magnetization data as a function of applied field perpendicular to the planes at several different temperatures. The curves have been vertically offset for better clarity and the arrows indicate the field sweep direction. All show a gradual increase in torque with a sharp first-order phase transition into the normal state, H_{c2}, at 4.97, 4.96 and 4.95 T at 20, 100 and 175 mK, respectively. A first-order phase transition in the perpendicular field orientation had been previously observed below 0.8 K [19]. The trace at the base temperature of 20 mK shows additionally a pronounced hysteretic feature around 2.5 T. This is indicative of vortex pinning effects and we interpret this feature as a vortex lattice peak effect at $H_p = 2.5$ T, as discussed in section 1. The peak effect shifts to $H_p = 2.2$ T at $T = 100$ mK, while it is completely absent above approximately 180 mK. This feature had originally been observed by Murphy *et al.* [20] and later Tayama *et al.* [21],

who suggested the possibility of a vortex lattice peak effect without further study. A vortex lattice peak effect is observed in most superconductors, including high-T_c, conventional and heavy fermion superconductors.

The peak effect in $CeCoIn_5$ disappears above $t_p = T/T_c = 0.08$, a rather low temperature when compared to other superconductors, where, for example, it was found to disappear above approximately $t_p = 0.4$ in $PrOs_4Sb_{12}$ [22], $t_p = 0.6$ in $Bi_2Sr_2CaCu_2O_{8+y}$ (BSCCO) [23], or $t_p = 0.8$ in $CeRu_2$ [24]. However, there is a noticeable trend between t_p and the defect structure of each material. While the $CeRu_2$ was a polycrystalline sample with Ru inclusions, the BSCCO and $PrOs_4Sb_{12}$ samples were single crystals with the difference that the BSCCO sample was overdoped. Obviously, the lower the defect density, the lower the peak temperature, t_p, confirming the pinning related origin of the feature. $CeCoIn_5$, on the other hand, is an undoped material that can be grown as high-purity single crystals. It can be seen from figure 1 that the peak effect occurs at $0.5H_{c2}$, which is far below the field where the PE is seen in conventional superconductors and is reminiscent of the situation encountered in high-T_c superconductors. One can view the vortex lines in $CeCoIn_5$ as stacks of loosely coupled pancake vortices, where both electro-magnetic and Josephson out-of-plane coupling are equally important. This is consistent with an estimated electronic anisotropy of $\varepsilon \sim 3$–4 as compared to $\varepsilon \sim 5$ in YBCO. For the most anisotropic high-T_c cuprates (e.g. BSCCO) with vanishing Josephson coupling the peak effect has been observed closer to the lower critical field, H_{c1}. We will comment further on the anisotropy issue below.

To obtain information about lattice disorder effects in $CeCoIn_5$, we show in the upper panel of figure 2 de Haas–van Alphen (dHvA) oscillations obtained by our torque magnetization technique at $T = 20$ mK in the field perpendicular orientation. A Fast Fourier Transform analysis is shown in the lower panel of figure 2 with several orbits indicated. The frequencies are in very good agreement with a previous dHvA analysis on $CeCoIn_5$ [25].

We utilize the Lifshitz–Kosevich formula and fit the amplitude, A, of the filtered frequency for the orbit F3 using $A(1/H) = A_0 \cdot R_T \cdot R_D$, where A_0 is a constant, R_T the reduction factor due to finite temperatures, $R_D \sim \exp(-T_D)$ the reduction factor due to impurity scattering, and T_D is the Dingle temperature [26]. Assuming an effective mass $m_{eff} = 8.4m_e$ [11], the fit yields $T_D = 0.33$ K, indicating very low broadening of the Landau tubes due to scattering. The Dingle temperature can be related to the scattering time, τ, *via* $T_D = \hbar/(2\pi k_B \tau)$, and the mean free path is $\ell = v_F \cdot \tau$, where k_B is the Boltzmann constant and v_F the Fermi velocity. From this information, the mean free path is estimated to be $\ell \approx 1870$ Å, which is extremely long and suggests a very low density of pinning centres that can naturally account for the rapid disappearance of the peak effect with temperature, as shown in figure 1. Eskildsen *et al.* [27] employed small angle neutron scattering (SANS) to investigate the vortex lattice structure in $CeCoIn_5$ in plane perpendicular fields. In an applied field of 2 T, they estimate the longitudinal vortex correlation length (straightness) to be roughly 100 vortex line spacings or 3 μm. They conclude that pinning is very weak in $CeCoIn_5$, in agreement with our findings.

Figure 3 shows the peak effect in more detail as observed at $T = 20$ mK in the plane perpendicular field orientation. The arrows indicate the direction of the field sweep (0.1 T/min) in increasing field starting at 0 T and reversing the sweep direction

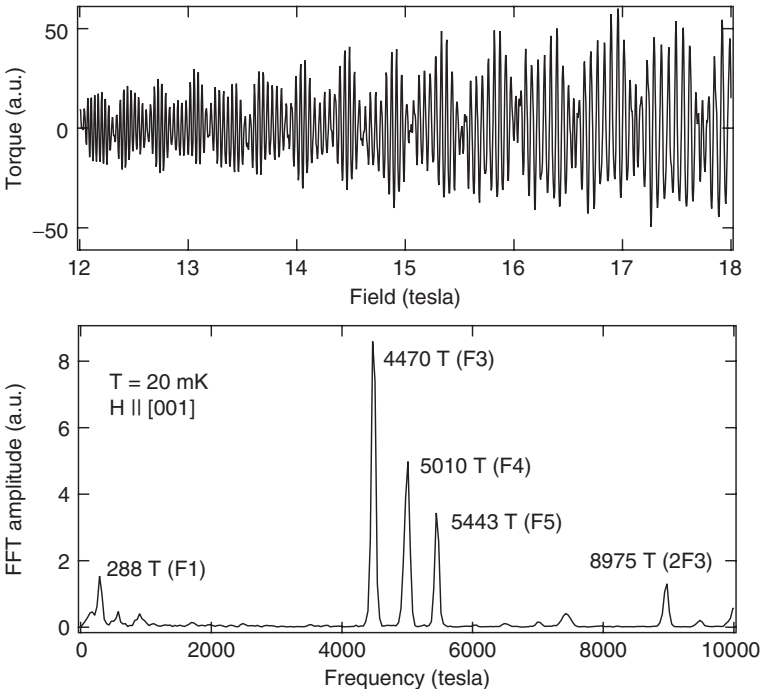

Figure 2. Upper panel: de Haas–van Alphen oscillations of $CeCoIn_5$ obtained at $T = 20$ mK with our torque cantilever for the plane perpendicular field orientation. Lower panel: Fast Fourier Transform of oscillations with indicated Fermi surface orbits F1, F3, F4, and F5 and corresponding frequencies.

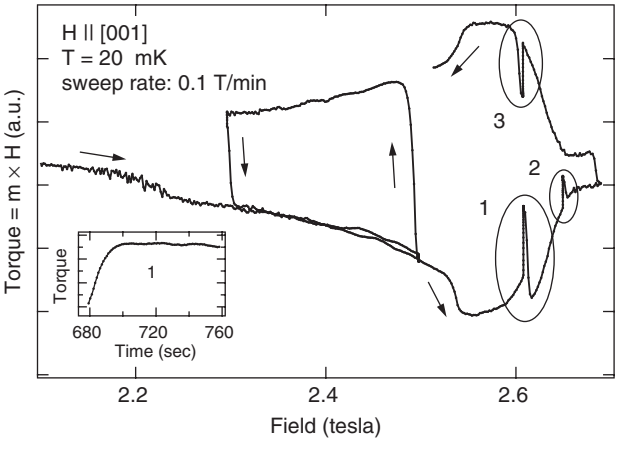

Figure 3. Torque versus field for perpendicular field orientation at $T = 20$ mK and magnet sweep rate 0.1 T/min. The arrows indicate the sweep direction with a minor loop between 2.3 and 2.5 T. The data points inside the three circled areas at 2.6 and 2.65 T were obtained after halting the sweep and recording the torque in the time domain (inset shows this for the area labeled with '1' as an example).

just below 2.7 T (the noise around 2.2 T originates from flux jumps within the superconducting magnet). Also shown is a minor loop between 2.3 and 2.5 T. The traces of the minor loop merge exactly with the magnetization after reversing the field at 2.7 T and sweeping back down. This indicates that the flux profile (induction) within the sample is fully inverted within 0.02 T, confirming the expected very weak pinning.

The data inside the three circled areas at 2.6 and 2.65 T were obtained after halting the sweep and monitoring the torque as function of time (this entire sweep was taken with time as the trigger parameter for data acquisition). It is evident in a plot of torque versus time (see inset to figure 3) that after a certain amount of time the signal saturates and becomes constant. This is the well-known flux relaxation or vortex creep phenomenon seen in many systems and previously also reported for $CeCoIn_5$ [28]. Within the classical Bean description of flux profiles inside superconductors, the slope of the flux profile is assumed to be constant throughout each half of the sample and to be proportional to the critical current density, $\partial B/\partial x \sim j_c$. After having ramped up the field and halted, vortices creep further into the centre of the sample, thereby decreasing the slope of the profile and, hence, the critical current density. Upon resuming the field ramp, the initial slope (or j_c) is reestablished. This phenomenological description fully accounts for the observed magnetization behaviour seen in figure 3. Close to the maximum of the PE the critical current is largest, yielding a stronger relaxation than at fields further away from the peak (note the opposite sign of the change in magnetization during the sweep down cycle, corresponding to a creeping of vortices out of the sample). Analogous results have recently been reported on $CeRu_2$ [24] and on V_3Si [29] obtained with SQUID magnetometry.

2.2. *Magnetization at different angles*

Figure 4 shows the torque as a function of field at $T = 20$ mK for different orientations of the applied field with respect to the conducting planes. Additionally, each panel depicts a cartoon of the anticipated vortex structure inside $CeCoIn_5$ at an angle of 90, 17 and 2° out of planes, respectively. The thick gray lines represent the conducting $CeIn_3$ layers, while the blank area in-between corresponds to the less-conducting $CoIn_2$ layers. The small black rectangles are pancake vortices and the black line parallel to the layers is a Josephson vortex (see also discussion about vortex structures in section 1).

The first obvious change is the increase of H_{c2} from 4.97 T at plane perpendicular (90°) to 11.57 T at 2°, reflecting the anisotropy of the material. Additionally, the width of the first-order transition increases by one order of magnitude, from 0.06 T at 90° to 0.66 T at 2°. One could refer to this as a change from a 'weak' to a 'strong' first-order phase transition at the upper critical field, H_{c2}. The upper panel shows data from figure 1 displaying a symmetric peak effect with respect to the sweep direction. The occurrence of the PE at field $0.5H_{c2}$ suggests a loosely coupled vortex pancake structure as sketched in the inset. This situation is reminiscent of the least anisotropic high-T_c cuprate YBCO. We observe similar behaviour in the PE at angles of 77, 62 and 47° (not shown). The middle panel of figure 4 shows the PE at fields 17°

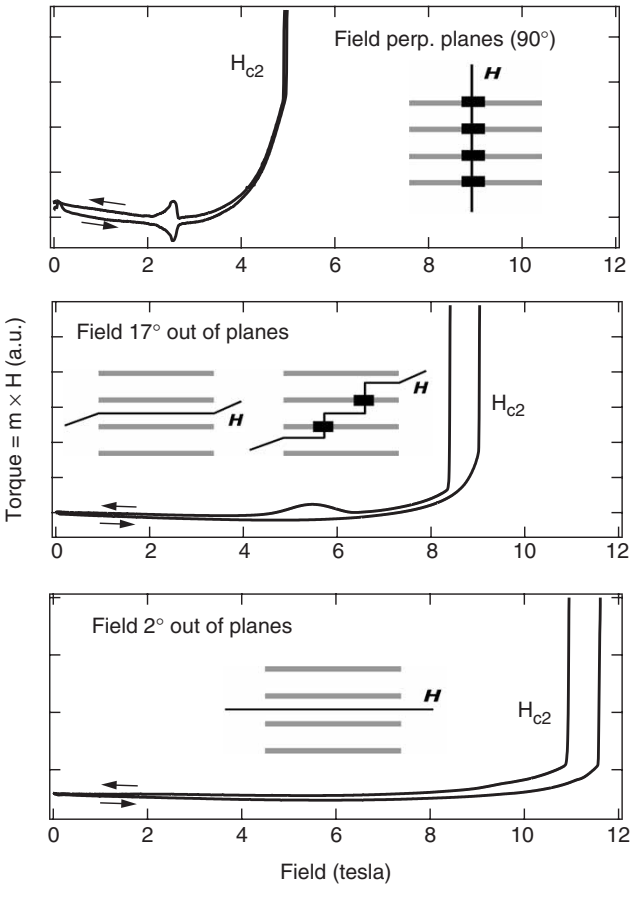

Figure 4. Torque as function of applied field at $T = 20\,\text{mK}$ for different field orientations. Upper panel: with field perpendicular to the planes a symmetric peak effect (PE) occurs; the vortex structure corresponds to a loosely coupled stack of pancake vortices. Middle panel: with fields at 17° out of the planes an asymmetric PE occurs; the induction is parallel to the planes in increasing field, while a kinked state forms in decreasing field. Lower panel: with fields at 2° no PE is detectable; the vortex structure corresponds to a pure Josephson vortex state.

out of the planes, displaying asymmetric behaviour with the PE completely absent for the sweep-up direction. An asymmetry is already visible at 32° angle (not shown). The proposed corresponding vortex structures are sketched in the inset. During the sweep-up half-cycle, the induction within the superconductor remains parallel to the conducting planes and at an angle to the applied field up to H_{c2}. The vortex structure consists of coreless Josephson vortices aligned parallel to the conducting planes (but not necessarily confined between two adjacent planes). The sweep-down second half-cycle starts out of the normal state, where the field penetrates the material. Upon entering the superconducting state, a kinked vortex structure forms, consisting of in-plane pancake vortices connected by Josephson vortices running between the planes (see also discussion in section 1). The bottom panel of figure 4 shows the

hysteresis cycle in the close-to-parallel field orientation, where the PE is absent for both sweep directions. Obviously, a 3-dimensional model with Abrikosov vortices fails to describe the data. We propose that the vortex structure here is a pure Josephson vortex state for both sweep directions. The absence of the PE suggests a complete absence of pancake vortices, as they are responsible for a decoupling transition leading to changes in the critical current and the occurrence of the peak effect. We observe identical angular behaviour on a second $CeCoIn_5$ sample originating from another batch of crystals from the same source. One might also consider an alternative explanation for our observed magnetization anomaly. In this scenario, the anomaly would not be caused by a peak effect, but rather induced by the proximity to a quantum critical point (QCP). However, most recent experimental results report about a magnetic-field-tuned QCP for both field orientations, perpendicular as well as parallel [30]. Our measurements show that the magnetization anomaly disappears at field orientations close to plane parallel and, hence, cannot be caused by the QCP in $CeCoIn_5$.

Vortex crossover scenarios are well known in the anisotropic high-T_c cuprates. Feinberg and Villard [31] derive theoretically a field-angle phase diagram, concluding that the region of stability of the parallel Josephson state increases with the anisotropy, ε, and the energy barrier height against generating a normal vortex core within the superconducting layer [31]. Hence, when the angle of an applied field exceeds a certain threshold value, the Josephson vortex state would transform into a kinked-lattice state. For fields on the order of several tesla at a given energy barrier height and a material with $\varepsilon = 5$ (YBCO), the threshold angle is predicted to be about 5° out of plane, while a material with $\varepsilon = 55$ (BSCCO) gives an angle of about 20°. Experimentally, vortex lock-in states were reported, for example, for $La_{1.9}Sr_{0.1}CuO_4$ [32], BSCCO [33], low-T_c $Mo_{77}Ge_{23}$/Ge multilayers [34], or the organic superconductor (BEDT-TTF)$_2$Cu(SCN)$_2$ [35]. Although the electronic anisotropy in $CeCoIn_5$ as derived from the ratio of reported effective masses is close to YBCO, the threshold angle seems much larger. We believe that the reasons for occurrence of the Josephson state over an extended range of angles, i.e. quasi-2D behaviour, in $CeCoIn_5$ are heavy electrons, large condensation energy and the now well-established paramagnetic limit. Recent X-ray absorption fine structure experiments on Sn-substituted $CeCoIn_5$ also clearly demonstrate the quasi-two-dimensional nature of superconductivity [36]. It was found that Sn substitutes preferentially onto the In sites within the Ce–In planes and readily destroys superconductivity at a level of only 3.6%. On the other hand, Rh-substitution onto the Co sites or La-substitution onto the Ce sites have a much weaker effect. The authors conclude that the superconducting state is confined within the Ce–In planes, consistent with a quasi-2D electronic structure.

We did not observe flux avalanches in any field orientation in the investigated temperature range $20\,\mathrm{mK} < T < 200\,\mathrm{mK}$. Avalanches have been observed using torque magnetometry, e.g. in the molecular superconductor κ-(BEDT-TTF)$_2$Cu(NCS)$_2$ in a wide range of angles and fields [18]. It is clear from our measurements that, at field angles close to the parallel orientation, all vortex activity ceases in $CeCoIn_5$, neither vortex avalanches nor a vortex lattice peak effect are present. We explain this with a crossover from an Abrikosov vortex state to a Josephson vortex state. The absence of Abrikosov vortices close to field parallel

orientations is consistent with the observation of a Fulde–Ferrell–Larkin–Ovchinnikov (FFLO) superconducting state that has been reported for $CeCoIn_5$ [37–43]. The FFLO state occurs only when orbital pair-breaking is not the dominant effect, which suggests that no Abrikosov vortices should form. A full rotational study of the FFLO state demonstrates that the FFLO signature disappears when the field is rotated by more than 15° out of the plane parallel field orientation [37, 42], an angle where the vortex peak effect re-emerges in our magnetization measurements.

3. Summary

In summary, we show that for magnetic fields parallel to the conducting layers in $CeCoIn_5$ no Abrikosov vortex signature is present, as demonstrated by the disappearance of the vortex lattice peak effect, which, however, is present for larger field angles up to the plane perpendicular orientation. We explain this with a crossover from the usual Abrikosov vortex lattice to a Josephson vortex lattice for parallel field orientations. The Pauli paramagnetic limit in $CeCoIn_5$, the large condensation energy and the heavy masses make it possible to achieve an Abrikosov vortex-free state with the field aligned parallel to the planes. Furthermore, we find no vortex avalanches for any field orientation. Thus, we conclude that the Josephson vortex state, together with an extraordinary long mean free path, is crucial for the formation of the spatially modulated Fulde–Ferrell–Larkin–Ovchinnikov superconducting state in $CeCoIn_5$.

Acknowledgments

This work was supported by the National Science Foundation under Cooperative Agreement No. DMR-0084173, an NHMFL In-House Research Program, the State of Florida, and the US Department of Energy. We would like to thank C. J. Olson and A. E. Koshelev for stimulating discussions about vortex behavior in anisotropic superconductors.

References

[1] G. Blatter, M.V. Feigel'man, V.B. Geshkenbein, *et al.*, Rev. Mod. Phys. **66** 1125 (1994).
[2] S.H. Autler, E.S. Rosenblum and K.H. Gooen, Phys. Rev. Lett. **9** 489 (1962).
[3] C.J. Olson, C. Reichhardt, R.T. Scalettar, *et al.*, Physica C **384** 143 (2003).
[4] J.R. Clem, Supercond. Sci. Technol. **11** 909 (1998).
[5] W.K. Kwok, J.A. Fendrich, C.J. van der Beek, *et al.*, Phys. Rev. **73** 2614 (1994).
[6] G. Blatter, V. Geshkenbein, A. Larkin, *et al.*, Phys. Rev. B **54** 72 (1996).
[7] A.E. Koshelev, Phys. Rev. B **68** 094520 (2003).
[8] See referenced articles in [7].
[9] C. Petrovic, P.G. Pagliuso, M.F. Hundley, *et al.*, J. Phys.: Condens. Matter **13** L337 (2001).

[10] J. Costa-Quintana and F. Lopez-Aguilar, Phys. Rev. B **67** 132507 (2003).
[11] R. Settai, H. Shishido, S. Ikeda, *et al.*, J. Phys.: Condens. Matter **13** L627 (2001).
[12] A.M. Clogston, Phys. Rev. Lett. **9** 266 (1962).
[13] J.W. Loram, K.A. Mirza, J.R. Cooper, *et al.*, Phys. Rev. Lett. **71** 1740 (1993).
[14] B. Andraka, J.S. Kim, G.R. Stewart, *et al.*, Phys. Rev. B **40** 11345 (1989).
[15] G. Sparn, R. Borth, E. Lengyel, *et al.*, Physica B **312/313** 138 (2002).
[16] Y. Bang and A.V. Balatsky, Phys. Rev. B **69** 212504 (2004).
[17] D.E. Farrell, J.P. Rice, D.M. Ginsberg, *et al.*, Phys. Rev. Lett. **64** 1573 (1990).
[18] M.M. Mola, S. Hill, J.S. Brooks, *et al.*, Phys. Rev. Lett. **86** 2130 (2001).
[19] A. Bianchi, R. Movshovich, N. Oeschler, *et al.*, Phys. Rev. Lett. **89** 137002 (2002).
[20] T.P. Murphy, D. Hall, E.C. Palm, *et al.*, Phys. Rev. B **65** 100514(R) (2002).
[21] T. Tayama, A. Harita, T. Sakakibara, *et al.*, Phys. Rev. B **65** 180504(R) (2002).
[22] P.C. Ho, N.A. Frederick, V.S. Zapf, *et al.*, Phys. Rev. B **67** 180508(R) (2003).
[23] S. Ooi, T. Shibauchi, K. Itaka, *et al.*, Phys. Rev. B **63** 020501(R) (2000).
[24] P.C. Ho, S. Moehlecke and M.B. Maple, unpublished (cond-mat/0301281).
[25] D. Hall, E.C. Palm, T.P. Murphy, *et al.*, Phys. Rev. B **64** 212508 (2001).
[26] D. Shoenberg, *Magnetic Oscillations in Metals* (Cambridge University Press, 1984).
[27] M.R. Eskildsen, C.D. Dewhurst, B.W. Hoogenboom, *et al.*, Phys. Rev. Lett. **90** 187001 (2003).
[28] H.A. Radovan, T.P. Murphy, E.C. Palm, *et al.*, J. Low Temp. Phys. **133** 377 (2003).
[29] G. Ravikumar, M.R. Singh and H. Kupfer, Physica C **403** 25 (2004).
[30] F. Ronning, C. Capan, A. Bianchi, *et al.*, Phys. Rev. B **71** 104528 (2005).
[31] D. Feinberg and C. Villard, Phys. Rev. Lett. **65** 919 (1990).
[32] Yu. V. Bugoslavsky, A.A. Zhukov, G.K. Perkins, *et al.*, Phys. Rev. B **56** 5610 (1997).
[33] H. Enriquez, N. Bontemps, P. Fournier, *et al.*, Phys. Rev. B **53** R14757 (1996).
[34] S. de Brion, W.R. White, A. Kapitulnik, *et al.*, Phys. Rev. B **49** 12030 (1994).
[35] P.A. Mansky, P.M. Chaikin and R.C. Haddon, Phys. Rev. Lett. **70** 1323 (1993).
[36] M. Daniel, E.D. Bauer, S.W. Han, *et al.*, Phys. Rev. Lett. **95** 016406 (2005).
[37] H.A. Radovan, N.A. Fortune, T.P. Murphy, *et al.*, Nature **425** 51 (2003).
[38] A. Bianchi, R. Movshovich, C. Capan, *et al.*, Phys. Rev. Lett. **91** 187004 (2003).
[39] H. Won, K. Maki, S. Haas, *et al.*, Phys. Rev. B **69** 180504(R) (2004).
[40] T. Watanabe, Y. Kasahara, K. Izawa, *et al.*, Phys. Rev. B **70** 020506(R) (2004).
[41] C. Capan, A. Bianchi, R. Movshovich, *et al.*, Phys. Rev. B **70** 134513 (2004).
[42] C. Martin, C.C. Agosta, S.W. Tozer, *et al.*, Phys. Rev. B **71** 020503(R) (2005).
[43] K. Kakuyanagi, M. Saito, K. Kumagai, *et al.*, Phys. Rev. Lett. **94** 047602 (2005).